

Article

Bamboo Scrimber's Physical and Mechanical Properties in Comparison to Four Structural Timber Species

Sarah Putri Sylvayanti, Naresworo Nugroho *  and Effendi Tri Bahtiar 

Forest Products Department, Faculty of Forestry and Environment, IPB University (Bogor Agricultural University), Bogor 16680, Indonesia

* Correspondence: nares@apps.ipb.ac.id

Abstract: Bamboo scrimber is a sustainable engineered material that overcomes natural round bamboo's various weaknesses. This study compared the bamboo scrimber's mechanical (strength, stiffness, and ductility) to timber. The results showed that scrimber's physical and mechanical properties are comparable, even superior, to wood, especially in compression. Scrimber has a higher density than timber. Its drier equilibrium moisture content indicates that scrimber is more hydrophobic than timbers. The maximum crushing strength ($\sigma_{c//}$), compressive stress perpendicular-to-fiber at the proportional limit ($\sigma_{cp\perp}$) and that at the 0.04" deformation ($\sigma_{c0.04\perp}$), shear strength ($\tau_{//}$), longitudinal compressive modulus of elasticity ($E_{c//}$), lateral compressive modulus of elasticity ($E_{c\perp}$), and modulus of rigidity (G) of scrimber are higher than those of timbers. Both scrimber's and timber's flexural properties (modulus of rupture (σ_b) and flexural modulus of elasticity (E_b)) are comparable. On the contrary, the tensile strength parallel-to-fiber ($\sigma_{t//}$) of scrimber is weaker than that of timber. Scrimber is high ductility ($\mu > 6$) when subjected to compression perpendicular-to-fiber, medium ductility ($4 < \mu \leq 6$) when subjected to compression parallel-to-fiber, and low ductility (brittle) when subjected to bending, shear, or tensile parallel-to-fiber. The higher ductility of scrimber may give an alarm and more time before failure than timbers. Timbers have brittle to lower ductility when receiving each kind of loading scheme. The ratio of shear modulus to strength (G/τ) and compression modulus to strength parallel-to-fiber ($E_{c//}/\sigma_{c//}$) strongly correlates with the ductility ratio. However, the ratio of the flexural modulus of elasticity to the modulus of rupture (E_b/σ_b) and the ratio of the modulus Young to compression stress perpendicular-to-fiber ($E_{c\perp}/\sigma_{cp\perp}$) do not strongly correlate to the ductility value.



Citation: Sylvayanti, S.P.; Nugroho, N.; Bahtiar, E.T. Bamboo Scrimber's Physical and Mechanical Properties in Comparison to Four Structural Timber Species. *Forests* **2023**, *14*, 146. <https://doi.org/10.3390/f14010146>

Received: 11 December 2022

Revised: 9 January 2023

Accepted: 9 January 2023

Published: 12 January 2023



Copyright: © 2023 by the authors. Licensee MDPI, Basel, Switzerland. This article is an open access article distributed under the terms and conditions of the Creative Commons Attribution (CC BY) license (<https://creativecommons.org/licenses/by/4.0/>).

Keywords: bamboo scrimber; biocomposite; building material; ductility; mechanical properties; sustainable construction

1. Introduction

Awareness of sustainability toward the environment is rising, especially regarding materials for structural applications. This awareness and advances in technology encourage the development of sustainable engineering materials. Sustainable engineering materials can be produced using wood [1–8], bamboo [9–18], other lignocellulosic materials [19,20], or their composite with conventional material [21]. Engineered bamboo products overcome various weaknesses in natural round bamboo so that bamboo can be promoted to a high-class material. There are several types of engineered-bamboo products for structural members, i.e., laminated bamboo [22,23], bamboo board [24–26], and reconstituted densified bamboo [27,28]. Reconstituted densified bamboo, also known as bamboo scrimber, is a composite bamboo made by crushing bamboo culms into bundles and then pre-treating using heat treatment and immersing in adhesive before the hot pressing process [29,30]. Unlike laminated bamboo, where the layers are arranged parallel, the strips/bundles arranged in bamboo scrimber are irregular. There are no layer boundaries in bamboo scrimber [31]. Bamboo scrimber has several advantages, such as raw material efficiency (the percentage

of the end product to the total raw material expended) of up to 80% [32], high resistance to biodegradation [33], higher heat storage and heat conduction properties and lower moisture absorption than timber [27], high density [34,35], and reliable mechanical strength. Bamboo scrimber is adequate for external applications such as deck flooring because of its extraordinary Janka hardness [32]. Bamboo scrimber structures could be combined using traditional furniture tenons and modern connections [36]. Sharma et al. [37] also mentioned that engineered products could create a standard homogenous and reduce variability among members.

In addition to its sustainability, the primary considerations in using bamboo and wood for structural members are the structural properties. In addition to strength and stiffness, ductility is an essential requirement and a preferable mechanical property in structural design. Ductile structures have a particular alternative of bearing capacity, i.e., large deformations occur before failure, that can be used to alert building occupants in case of an unexpected load. Regarding robustness, ductility is desirable because it is widely assumed that a flexible structure may be more reliable and robust than brittle structures. Kirkegaard et al. [38] evaluated the robustness of a timber truss structure. The result of the model with ductile timber behavior shows that the robustness index is higher for these ductile elements. The building designers shall consider the ductile behavior, especially for structures in seismic areas. The classifications of ductility can be found in Eurocode 8: EN-1998-1 [39]. The importance of ductility design in structures relates to dynamically loaded structures in their application, e.g., design structures for bridges [40], wall panels on CLT houses [41,42], and light-frame buildings [43].

Bamboo has good strength, stiffness, and ductility that enable it to be used in situations requiring the material's ability to undergo considerable deformation [44]. Different researchers have expressed the ductility index on a different quantitative basis. It can be expressed as energy absorption [45], curvature ratio [46,47], rotation ratio [48], and displacement ratio [49]. Ductility, in general definition, is the ratio between the ultimate and yield displacement. However, the timber yield criterion needs to be clarified, as it is for example, for steel structures. There are also different methods for determining the yield point of timber structures. The value of yield displacement can vary up to 80% depending on the method used [50]. Although scrimber has a similar appearance and form to wood and wood-based products, its fundamental composition and ultimate fracture differ [51]. Experimental studies on its mechanical properties, including ductility and its comparison to structural wood, may significantly contribute to the scrimber utilization for green construction members. Further research is necessary to characterize scrimber structural properties.

2. Materials and Methods

2.1. Materials

Bamboo scrimber used in this study were commercially produced by Bambulogy, a building design company in Tangerang, Indonesia. The supplied scrimber had dimensions of 30 mm × 140 mm × 1870 mm. Scrimber used in this study was manufactured by mixing a few species of bamboo, including hitam (*Gigantochloa atrovioleacea*), tali (*Gigantochloa apus*), mayan (*Gigantochloa robusta*), and gombong (*Gigantochloa pseudoarundinacea*), which have diameters range between 7 and 12 cm. The manufacturing procedures were as follows:

- a. Natural round bamboo was split into 3–8 parts and cut longitudinally into 2.5 m lengths.
- b. The outer skin and inner part were removed using an expanding machine, then crushed and flattened.
- c. The strands were carbonized for 2–3 h at 190 °C to remove extractive components in natural bamboo. After the carbonization process, the strands become less stiff and are easier to form the scrimber because their modulus decreases when more than 150 °C temperature is applied.

- d. The dry carbonized strands, having a moisture content of 0% (zero percent), were placed in the 65 °C temperature tunnel for 3.5 h until the moisture content increased and reached 0.5%.
- e. The adhesive used in this manufacturing process was phenol-formaldehyde (PF). The adhesion process was performed by dipping strands in PF adhesive solution (PF:water = 1:1) for 10 min, and then draining it.
- f. Strands coated with adhesive were dried at 70 °C for 2–4 h until they reached the target moisture content of 11%.
- g. After drying the resin-coated strands, the cold pressing process was carried out for 2 min with a compression load of 687 kN, equivalent to 2.625 MPa pressure.
- h. Next, blocks were formed in molds over 12 h using a hot curing machine with several temperatures in three parts of time, namely 110 °C for 3 h, 135 °C for 6 h, and 120 °C for 3 h. A 598–638 N load was applied to the beam during the molding process.
- i. Conditioning for three weeks, the last stage, releases the residual stress.

In addition to bamboo scrimber, the material used in this study included sawn lumber of red meranti (*Shorea* sp.), mahogany (*Swietenia* sp.), agathis (*Agathis* sp.), and pine (*Pinus* spp.) purchased from timber markets in Bogor, West Java-Indonesia as comparisons. Further, the bamboo scrimber and timbers were cut into specimens based on the standard requirement for testing of mechanical properties, ASTM D143 *Standard Test Methods for Small Clear Specimens of Timber* [52]. The specimen sizes are given in Table 1 and Figure 1. All specimens were air-dried in indoor environmental conditions for a month to reach equilibrium moisture content.

2.2. Methods

2.2.1. Physical Properties

The width (b) and depth (d) of small-clear size specimens were measured using a digital caliper with an accuracy of 0.01 mm. A digital caliper was employed to measure specimen length (L) when less than 150 mm; a ruler was used to measure the longer specimen. Specimen mass was weighed at the air-dry moisture content before the mechanical properties test (m_0). Not long after the mechanical properties test, the specimen's stringy part was removed, then the mass was weighed (m_1). The specimens were placed in a 102 ± 3 °C oven for 48 h; after this, they were weighed every three hours and placed in the oven again until the mass was constant at three consecutive weights (m_2). The moisture content (M_c), density (ρ), and specific gravity (G_b) were calculated following Equations (1a)–(1c).

$$M_c = \frac{m_1 - m_2}{m_2} \times 100\% \quad (1a)$$

$$\rho = \frac{m_0}{V} = \frac{m_0}{Lbd} \quad (1b)$$

$$G_b = \frac{\rho}{(1 + M_c\%)\rho_{\text{water}}} \quad (1c)$$

Table 1. Experimental test methods for bamboo scrimber and timber.

Test Method	Direction	Number of Specimen (n)		Specimen Size (b cm \times d cm \times L cm)		Loading Rate (mm/min)
		Scrimber	Timber	Timber	Scrimber	
Tension	Parallel-to-fiber	14	50	2.5 \times 2.5 \times 46 (Figure 1a)	2.5 \times 2.5 \times 46 (Figure 1a)	1.00
Compression	Parallel-to-fiber	9	50	2.5 \times 2.5 \times 10 (Figure 1b1)	3 \times 3 \times 20 (Figure 1b2)	0.30
Compression	Perpendicular-to-fiber	7	50	5 \times 5 \times 15 (Figure 1c1)	3 \times 3 \times 15 (Figure 1c2)	0.305
Shear	Parallel-to-fiber	7	50	5 \times 5 \times 6.3 (Figure 1d1)	3 \times 5 \times 6.3 (Figure 1d2)	0.6
Bending	Center point loading	10	50	2.5 \times 2.5 \times 41 (Figure 1e)	2.5 \times 2.5 \times 41 (Figure 1e)	1.3

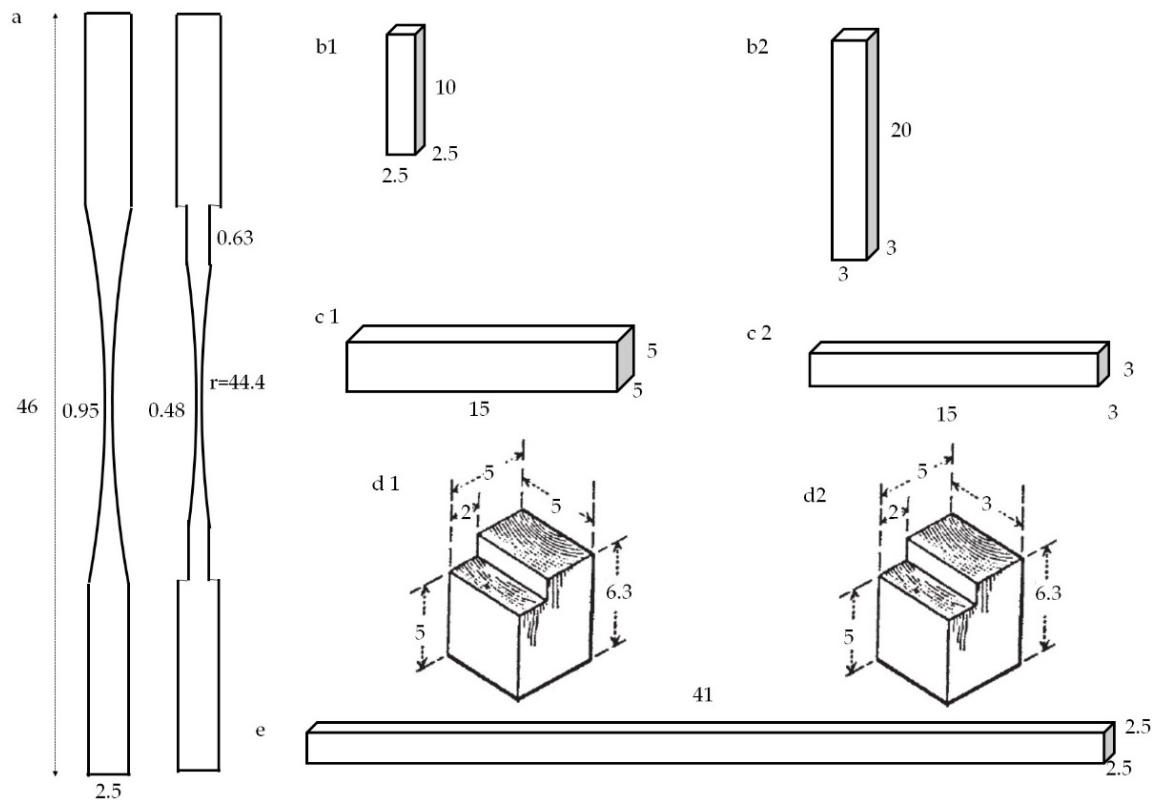


Figure 1. Timber and scrimber specimens for tensile test parallel-to-fiber (a), timber (b1) and scrimber (b2) specimens for compressive test parallel-to-fiber, timber (c1) and scrimber (c2) specimens for compressive test perpendicular to fiber, timber (d1) and scrimber (d2) specimens for shear test, timber and scrimber specimens for bending test (e). (Note: the size unit is cm).

2.2.2. Mechanical Properties

Mechanical properties (including flexural, compression, tensile, and shear) were tested based on ASTM D143 [52] using a SATEC/Baldwin Universal Testing Machine (UTM) 30-ton capacity (SATEC/Baldwin, Grove City, PA, USA), equipped with periodically calibrated load cell, linear variable displacement transducers (LVDT), and multipurpose digital indicator (MPDI) data acquisition machine (installed by PT Testindo, Jakarta and calibrated by PT Global Quality Indonesia, Bandung, ID) [5], and UTM Instron type 3369 (PT Patochemi Murni Aditama, Jakarta, ID). The test methods, specimens, and parameters are summarized in Table 1. The flexural modulus of elasticity (E_b), modulus of rupture (σ_b), compression strength perpendicular-to-fiber ($\sigma_{c\perp}$), compression stress parallel-to-fiber ($\sigma_{c\parallel}$), the Young modulus parallel- and perpendicular-to-fiber ($E_{c\parallel}$ and $E_{c\perp}$), tensile strength parallel-to-fiber ($\sigma_{t\parallel}$), shear strength (τ_{\parallel}), and shear modulus (G) were calculated following equations in Table 2. The elastic properties (including modulus of elasticity (E_b , $E_{c\parallel}$, and $E_{c\perp}$) and shear modulus (G)) were calculated as the slope of the linear (proportional) part of the load-deformation or stress-strain diagram.

2.2.3. Ductility Ratio

Ductility expresses the ratio between ultimate displacement (Δ_u) and yield displacement (Δ_y) (Equation (2)). The Δ_u and Δ_y are commonly obtained from tensile and compressive tests. However, this study measured ductility ratio (μ) through several mechanical property tests (i.e., tension parallel-to-fiber, compression parallel-to-fiber, compression perpendicular-to-fiber, shear parallel-to-fiber, and bending).

$$\mu = \frac{\Delta_u}{\Delta_y} \quad (2)$$

Table 2. Equations used to determine mechanical properties of timber and bamboo scrimber.

Mechanical Properties	Equations
Modulus of Elasticity (E_b)	$E_b = \frac{PL^3}{4\Delta bh^3}$
Modulus of Rupture (S_R)	$\sigma_b = \frac{3P_{max}L}{2bh^2}$
Tension Parallel-to-fiber Strength ($F_{t\parallel}$)	$\sigma_{t//} = \frac{P_{max}}{A}$
Compression Parallel-to-fiber Strength ($F_{c\parallel}$)	$\sigma_{c//} = \frac{P_{max}}{A}$
Compression Perpendicular-to-fiber Strength at Proportional Limit ($F_{cp\perp}$)	$\sigma_{cp\perp} = \frac{P_p}{A}$
Compression Perpendicular-to-fiber Strength at 0.04 inch ($F_{c0.04\perp}$)	$\sigma_{c0.04\perp} = \frac{P_{0.04}}{A}$
Compression modulus (E_c)	$E = \frac{\sigma}{\epsilon}$
Shear Parallel-to-fiber Strength (F_s)	$\tau_{//} = \frac{P_{max}}{A}$
Shear Modulus (G)	$G = \frac{\tau}{\gamma}$

To estimate ductility, the determination of a yield point is necessary. Since the yield criterion for timber is not well-defined (as it is for example, for steel structures), different methods for determining the yield displacement for timber connections or structures exist (Figure 2). This timber yield point is known as the pseudo-yield point. Some well-known procedures utilized in this research are:

- Karacabeyli and Ceccotti (K&C) [53]: The yield point in this method is viewed as the point on the load-deformation curve equal to 50% of the maximum capacity (Figure 2a).
- Commonwealth Scientific and Industrial Research Organization (CSIRO) [54]: In this case, the yield point in this method is viewed as the point on the load-deformation curve corresponding to 40% of the maximum capacity. The 40% of the maximum deformation is adjusted by a factor of 1.25. The point on the load-deformation curve formed by the intersection of the projection line and the new coefficient of displacement value is viewed as the yield point, and the yield load is determined (Figure 2b).
- European Committee for Standardization (CEN) [55]: This method uses the secant and tangent lines of the two parts of the load-deformation curve to determine the yield point. The first line indicates the initial stiffness, calculated from 10% to 40% of the maximum load. The angle between the secant line and displacement axis is α . The slope of the second line is equivalent to one-sixth (1/6) of the slope of the second of the load-displacement curve. The yield point is resolved as the intersection of the first and second lines (Figure 2c).
- Yasumura and Kawai (Y&K) [56]: The secant line between 10% and 40% of the maximum load indicates the initial stiffness. A line connecting the data point of 40% and 90% of the peak load, called a chord line, is drawn. Then a line parallel to the chord line and tangent to the load-deformation curve is created. The last line represents the post-elastic area before the maximum load. The intersection point between the initial stiffness and tangent line is projected horizontally onto the load-displacement curve to obtain the yield point displacement (Figure 2d).
- Equivalent Energy Elastic-Plastic (EEEP) [57]: In this method, a bilinear curve represents an assembly's perfect elastic-plastic curve (Figure 2e). The area under the load-displacement curve ($W_{failure}$) is assumed to be the same as the area beneath the bilinear curve. Initial stiffness in this method corresponds to the first straight line, which is defined as being between 0% and 40% of the peak load (K_{40}). Deformation at failure ($\Delta_{failure}$) is defined as deformation at 80% of maximum load. The following equation is used to calculate the yield load (P_y) is Equation (3).

$$P_y = \left[\Delta_{failure} - \sqrt{\Delta_{failure}^2 - \frac{2W_{failure}}{K}} \right] \times K \tag{3}$$

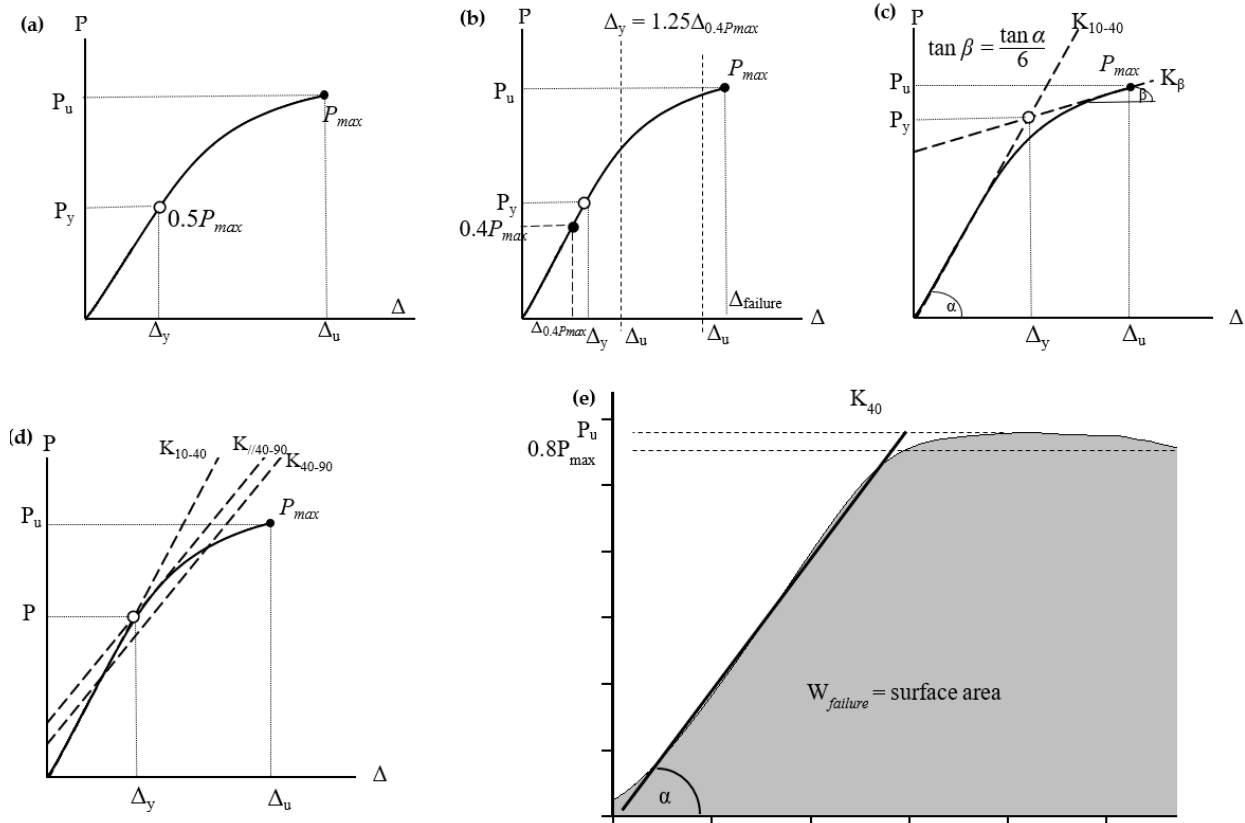


Figure 2. Methods used to obtain yield point: (a) Karacabeyli and Cecceotti; (b) CSIRO; (c) CEN; (d) Yasumura and Kawai; and (e) Equivalent Energy Elastic-Plastic Curve (EEEP).

2.2.4. Analysis

The ductility ratio of all specimens tested is presented using descriptive statistics, including mean, standard deviation, minimum and maximum value. Simple linear regression analysis was conducted to analyze the relationship between ductility ratio and stiffness to strength ratio.

3. Results and Discussion

3.1. General Description of Bamboo Scrimber

The bamboo scrimber used in this study is a board similar to sawn timber. Scrimber has a smoother and flatter surface than timber. Its color is brown to dark brown due to the treatments during the manufacturing process. Unlike other common wood composites, scrimber has no layers, while the others, such as plywood and glued laminated timber/bamboo, have multi-layers. The fiber surface type of scrimber is stranded [58]. This stranded type gives a more natural look. Compared to timber, scrimber is not a lightweight material due to its high density, which may raise problems in transportation.

3.2. Physical Properties

Physical properties tested include moisture content (M_c), density (ρ), and specific gravity (G_b). Moisture content is crucial, especially on hygroscopic materials, because it affects their volume and mass, affecting other properties. The average moisture content of all specimens from this experimental study ranged between 8.14% and 15.46% (Figure 3), similar

to the previous reports on wood [4,5,8], wood products [59,60], and bamboo [10–14,61] conducted in Bogor, West Java (ID). This equilibrium moisture content is wetter than bamboo in sub-tropical regions such as Coventry (UK) [15,16]. The scrimber's equilibrium moisture content is $(8.14 \pm 0.34\%)$, generally drier than wood. As hygroscopic material, scrimber's air-dry moisture content is still higher than mortar [21]. Scrimber had the lowest moisture content, while pine had the highest one. Scrimber, as an engineered product, has undergone a series of processes, including drying, pressing, and gluing, which causes this material to be more hydrophobic than untreated wood. The bonding process using phenol-formaldehyde (PF) resin reduces the water absorption ability. PF resin adhesive is commonly applied for outdoor products, so it can excellently resist the environment's humidity fluctuation.

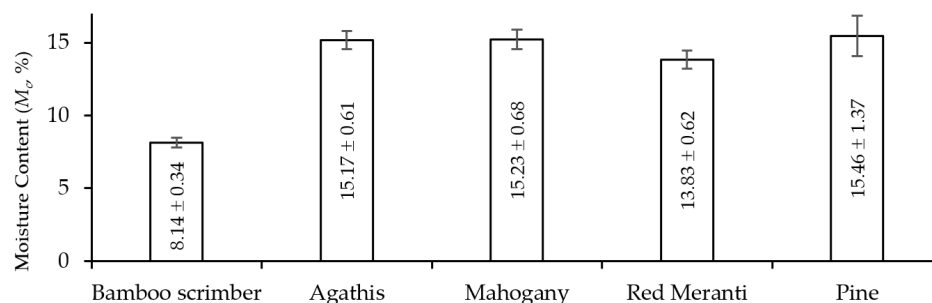


Figure 3. Air-dried moisture content of all specimens.

The scrimber and timber's average density and specific gravity are presented in Figure 4. The density varies between 0.46 and 0.98 g/cm^3 . The specific gravity (G_b) is determined based on oven-dried mass and air-dried volume. The G_b values range between 0.40 and 0.90. In both cases, agathis has the lowest value, while scrimber is the densest. Both scrimber and timber are hygroscopic materials that absorb water from their surrounding environment; thus, their masses relate to moisture content. The higher G_b value means the total hollow cavity volume decreases; this explains the scrimber's lower moisture content than timber. The scrimber is denser than the other timbers. The lower moisture content of scrimber also indicates the less available void for free water [62].

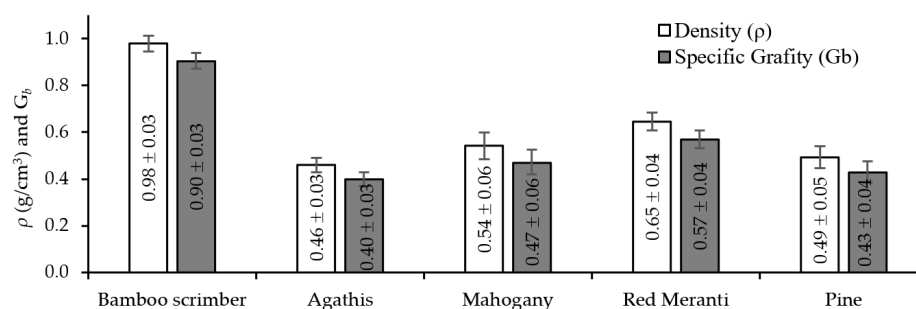


Figure 4. Density (ρ) and specific gravity (G_b) of all specimens.

3.3. Mechanical Properties

3.3.1. Tension Parallel-to-Fibers

The mean value for tension strength parallel-to-fiber of the scrimber is 34.27 MPa (Table 3). This value is lower than Kumar et al.'s report [35], which equals 111 MPa for scrimber. The tensile strength parallel-to-fiber of the scrimber is the weakest among other materials, while the strongest was red meranti (128.48 MPa). Bamboo scrimber used in this study was not flattened and crushed using an excellent machine for the defibering process but the simple manual one. It will cause the bamboo strips to not have well-maintained fiber direction longitudinally. At the same time, it is supposed to be horizontally maintained to decrease the mechanical properties, especially in tension parallel to the fiber. Huang et al. [36] reported

that early defibering was mainly hand-made, using manual hammering and roll-in. However, the former method could cause mechanical damage to bamboo. Figure 5a shows a sample of the load-displacement curve in tension test parallel-to-fiber of each material. The load-displacement curves generally had a linear relationship with increasing load until the final failure. Thus, the proportional limit is near the ultimate load. Failures found in scrimber specimens are along with the bamboo fiber (Figure 5b).

Table 3. Mechanical property test results for bamboo scrimber and timber specimens.

Mechanical Properties (MPa)	Scrimber (Mean \pm s)	Agathis (Mean \pm s)	Mahogany (Mean \pm s)	Red Meranti (Mean \pm s)	Pine (Mean \pm s)
Flexural modulus of elasticity (E_b)	8525 \pm 1275	6968 \pm 618	8033 \pm 1079 *	11002 \pm 1379 *	7218 \pm 1837 *
Modulus of rupture (σ_b)	71.14 \pm 9.85	52.08 \pm 4.49	70.47 \pm 11.37 *	72.42 \pm 12.15 *	55.15 \pm 10.18 *
Tensile strength parallel-to-fiber ($\sigma_{t\parallel}$)	34.27 \pm 16.37	61 \pm 19.30	74.94 \pm 21.21	128.48 \pm 35.68	72.56 \pm 28.68
Compressive strength parallel-to-fiber ($\sigma_{c\parallel}$)	64.85 \pm 4.40	24.75 \pm 2.86	30.67 \pm 5.36	40.84 \pm 6.46	29.07 \pm 4.07
Compressive modulus of elasticity parallel-to-fiber ($E_{c\parallel}$)	5296 \pm 577	1552 \pm 275	2030 \pm 376	2617 \pm 452	2048 \pm 335
Compressive stress perpendicular-to-fiber at proportional limit ($\sigma_{cp\perp}$)	19.60 \pm 3.00	4.05 \pm 0.88	7.76 \pm 1.25	5.41 \pm 0.75	5.11 \pm 1.27
Compressive stress perpendicular-to-fiber at 0.04" deformation ($\sigma_{c0.04\perp}$)	21.31 \pm 4.80	3.77 \pm 0.65	7.08 \pm 1.10	5.06 \pm 0.65	5.02 \pm 1.10
Compressive modulus of elasticity perpendicular-to-fiber ($E_{c\perp}$)	980.4 \pm 58.2	194.7 \pm 40.4	341.4 \pm 46.8	243.3 \pm 35.8	241.2 \pm 50.0
Shear strength (τ_{\parallel})	11.15 \pm 2.50	7.09 \pm 1.48	9.88 \pm 1.24	8.74 \pm 1.41	8.48 \pm 1.59
Shear modulus (G)	290.8 \pm 66.3	206.6 \pm 57.7	266.0 \pm 57.5	261.6 \pm 60.4	242.2 \pm 66.3

Note: s = standard deviation, * The flexural test of mahogany, red meranti, and pine was conducted by Bahtiar et al. [4], and then we recalculated them.

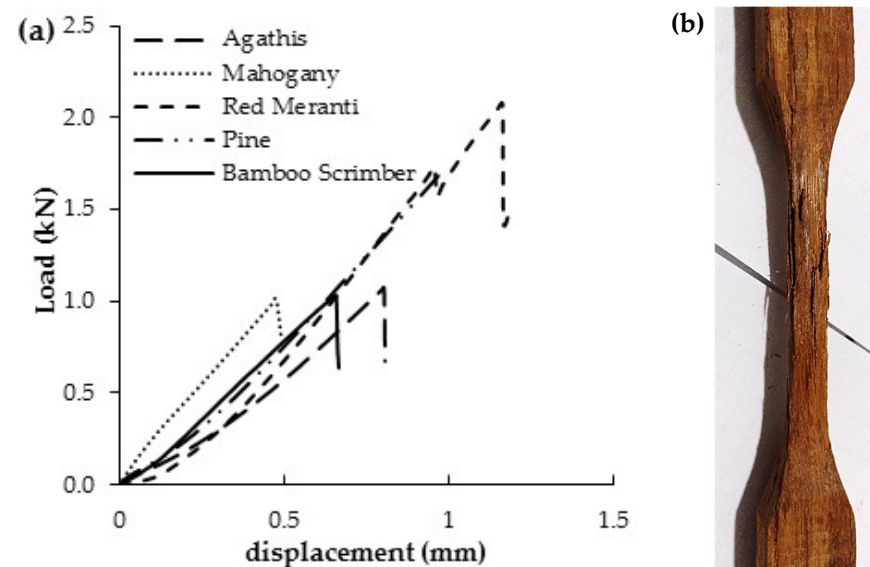


Figure 5. Tension parallel-to-fiber (a) results and (b) specimen failures in scrimber.

This failure type of scrimber in tension parallel-to-fiber was splintering tension. The failure type found in this study differs from the experimental study by Huang [63] and Sharma [37]; the failure mode of engineered bamboo is similar to wood in that the tension test is brittle, with the fibers fractured. The difference in failure between scrimber and timber loaded in tension parallel-to-fiber is that the fibers separate in scrimber, then fracture as the final failure at maximum load. While in timber, the fiber did not separate but was immediately fractured.

3.3.2. Compression

The scrimber's mean value of the compressive strength parallel-to-fiber is 64.85 MPa (Table 3). At the same time, the mean value of compressive stress perpendicular-to-fiber

at the proportional limit and 0.04-inch deformations are 19.60 and 21.31 MPa. Both compression strength parallel-to-fiber and compression stress perpendicular-to-fiber values are lower than Li et al.'s study [64], which equals 100.9 and 52.8 MPa, respectively. This compressive property's low value might be attributed to the scrimber's lower density than that of Li et al. The scrimber's density (ρ) in this study is 980 kg/m^3 , while the density in Li et al. is 1254 kg/m^3 [64]. However, the compression strength of bamboo scrimber in this experimental study is equivalent to laminated bamboo studied by Sharma [37], with values of 77 MPa for parallel-to-fiber and 22 Mpa for perpendicular-to-fiber.

The compressive strength parallel-to-fiber is three times stronger than the compressive strength perpendicular-to-fiber because the bamboo fibers' strength is higher in the parallel direction [35] than in the lateral direction. Scrimber's compressive strengths in this study, both parallel- and perpendicular-to-fiber, are higher than those of timbers. Scrimber is an engineered material composed of compressed bamboo fiber bundles arranged in parallel. As a result, the scrimber can withstand a high load applied to the bamboo fibers (Figure 5a). Timber loaded in compression perpendicular-to-fiber cannot reach the ultimate load, while bamboo scrimber can reach the ultimate load (Figure 6a).

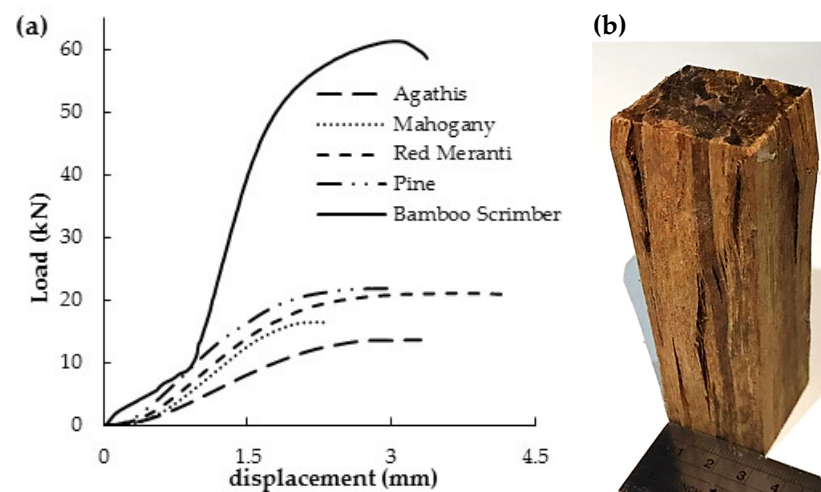


Figure 6. Compression parallel-to-fiber (a) results and (b) specimen failures in scrimber.

The scrimber's compressive modulus of elasticities parallel and perpendicular-to-fiber are 5296 and 980 MPa. While the timber's compressive modulus of elasticities parallel- and perpendicular-to-fiber range between 1552–2616 MPa and 195–341 MPa. Similar to the compressive strength value, the scrimber's compressive modulus is lower than the one reported by Li et al. [65], which were reported as 14,160 MPa for parallel-to-fiber and 4313 MPa for perpendicular-to-fiber.

Figures 6a and 7a show the load-displacement curves of the scrimber specimen under compression parallel- and perpendicular-to-fiber. Compared to the compression test parallel-to-fiber, all materials tested have a low compressive strength perpendicular-to-fiber. According to the load-displacement curve, the scrimber received twice the load with a similar displacement before failure to other materials tested. Therefore, scrimber has a higher compressive strength perpendicular and parallel-to-fiber than timber. The failure mode in compression parallel-to-fiber was buckling (Figure 6b).

In contrast, the bamboo fiber fracture is the failure mode of scrimber tested in compression perpendicular-to-fiber (Figure 7b). Li et al. [66] and Sharma et al. [37] also have similar buckling failure modes in laminated bamboo and scrimber. Fracture along the bamboo fiber in scrimber specimens indicates the bonding between bamboo fibers are the main weakness in terms of mechanical properties. Compression perpendicular-to-fiber failure is also found on the glue line.

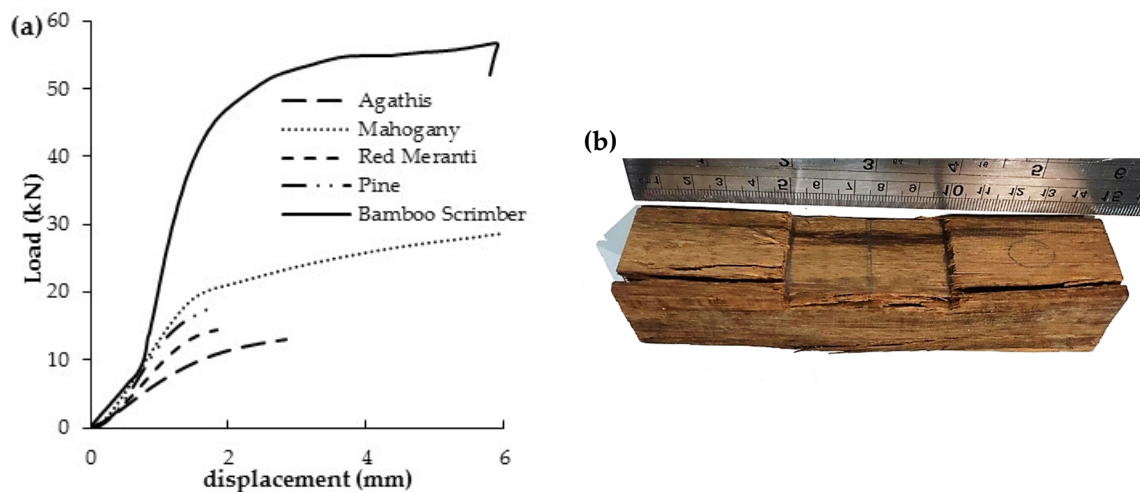


Figure 7. Compression perpendicular-to-fiber (a) results and (b) specimen failures in scrimber.

3.3.3. Shear

The shear strength of scrimber describes the bonding behavior between strands and adhesive [67]. Inter-fiber bonds greatly influence the shear strength within the bundle of fibrils of the bamboo culm. The shear strength value for scrimber ranges between 7.37 and 14.11 MPa, with a mean value of 11.15 MPa (Table 3). This mean value is similar to Kumar et al.'s [35] study, which equals 11.89 MPa for scrimber with slightly higher density (1.05 g/cm^3) than this study (0.98 g/cm^3). Scrimber has a higher shear strength than the timber. The shear strength value of the timber specimen ranges between 7.09 and 9.88 MPa. The highest shear strength value of timber was mahogany. Like the shear strength value, the highest shear modulus (G) of all specimens tested in this experimental study belonged to the scrimber, which equals 290 MPa. The failure type of scrimber can be seen in Figure 8b. Cracks along the main shear line split the specimen into two parts.

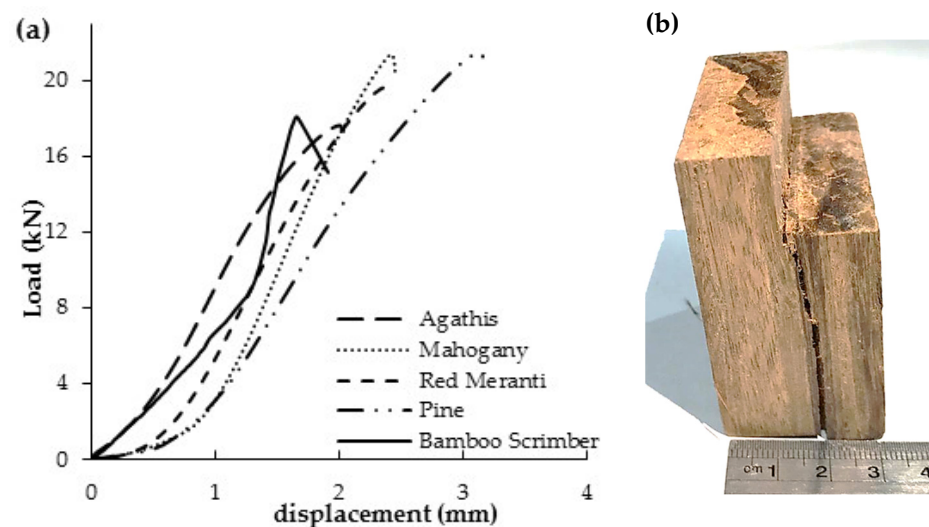


Figure 8. Shear parallel-to-fiber (a) results and (b) specimen failures in bamboo scrimber.

3.3.4. Bending

The scrimber's mean values for modulus of elasticity and modulus of rupture are 8525 MPa and 71.14 MPa, respectively (Table 3). This elastic modulus value is comparable to Li et al.'s [64] report, which equals 9199 MPa for a scrimber with high density (1.25 g/cm^3). However, the elastic modulus of scrimber in this experimental study is higher than Moso

bamboo studied by Chen et al. [44], which is equal to 10,470 MPa. However, the scrimber's modulus of rupture is lower than Moso bamboo, which equals 145.71 MPa.

The mean values for elastic and rupture modulus of timber are 6.97–11.00 GPa and 52.08–72.42 MPa. Red meranti had the highest value for elastic and rupture modulus of all specimens tested. Figure 9a shows the load-displacement curve of scrimber under flexural test. It shows that the scrimber specimen has reached maximum load with a relatively small displacement compared to other materials tested.

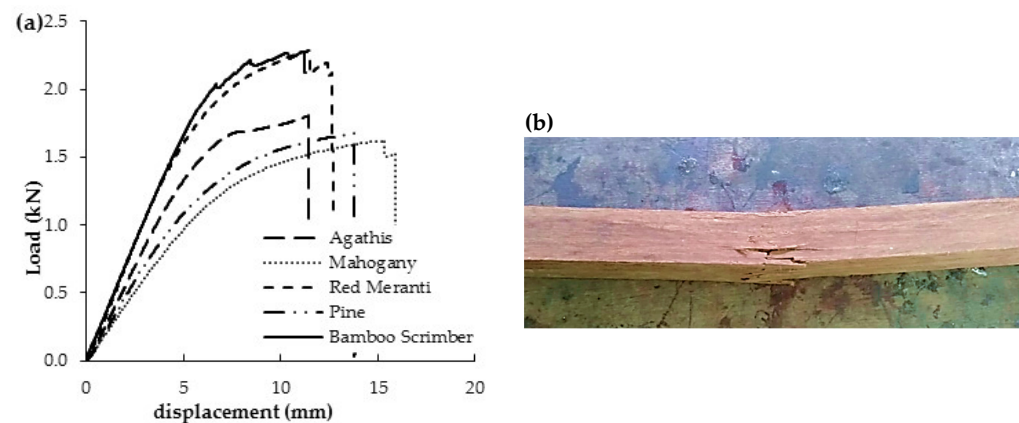


Figure 9. Flexural test (a) results and (b) specimen failures in bamboo scrimber.

The failure of scrimber appeared as a small crack in the middle part of the specimens (Figure 9b). This typical pattern of failure is commonly named ‘simple tension’ according to Bodig and Jayne [68]. Simple tension is not a common bending failure, especially in high-density wood. A similar failure mode was also found by Zou et al. [31]; the failure of all scrimber specimens occurred at the bottom of the mid-span. The typical failure mode is fiber fracture caused by tensile force.

3.4. Ductility Ratio

Eurocode 8 [39] defines ductility as the “ratio of the ultimate deformation and the deformation at the end of elastic behavior”. Although the definition of ductility is well-defined, the definition of yield point has yet to reach an international agreement [69]. Four different methods to determine yield points were used in this study, as mentioned above. Table 4 lists the descriptive statistics of ductility ratio (μ) determined from various procedures to obtain yield points. For tension, shear, and compression parallel-to-fiber tests, the yield point procedure based on CEN and Y&K methods cannot be determined, although these methods are bilinear methods, which should help balance the yield load according to the shape of the curve [50]. In this experimental study, the K_{10-40} line is located off the load-displacement curve causing the yield point to be undetermined for the examples shown in Figure 10. In contrast, in bending and compression perpendicular-to-fiber, the yield points can be obtained using four methods (i.e., K&C, CSIRO, CEN, and Y&K). Jorrisen and Fragiacomio [70] reported that for statically determined structures, ductility results in large local displacements such as compression perpendicular-to-fiber at the supports, compression at a certain angle in the wood-working joint, or large deformation in connection. However, yield points obtained using the EEEP method in timber also cannot be determined because, in timber, load-displacement curves do not have enough slip. The slip in this method tends to be very important to obtain deformation at failure ($\Delta_{failure}$), defined as deformation at 80%. This behavior is also found in the tension parallel-to-fiber test of scrimber. It can be seen that scrimber, as material construction occurs, slips before it fails.

Table 4. Descriptive statistic of ductility ratio.

Materials		Methods														
		K&C			CSIRO			CEN			Y&K			EEEP		
		<i>n</i>	Mean	<i>s</i>												
Bamboo scrimber	σ_b	10	2.7	0.4	10	2.6	0.3	10	1.5	0.2	10	2.2	0.4	10	1.53	0.18
	$\sigma_{c\parallel}$	9	3.5	0.4	9	4.3	0.5				9	1.78	0.20			
	$\sigma_{c\perp}$	7	9.5	3.7	7	10.2	4.8	7	6.7	2.9	7	7.0	2.3	7	5.15	1.90
	τ_{\parallel}	7	1.5	0.2	7	1.8	0.3				5	1.24	0.51			
	$\sigma_{t\parallel}$	14	2.0	0.3	14	1.9	0.3									
Agathis	σ_b	50	3.3	0.3	50	2.6	0.3	50	1.9	0.2	50	2.8	0.4			
	$\sigma_{c\parallel}$	50	3.1	1.1	50	2.9	1.0									
	$\sigma_{c\perp}$	50	3.2	0.5	50	3.2	0.5	50	1.8	0.4	48	2.4	0.7			
	τ_{\parallel}	50	2.4	0.5	50	2.4	0.5									
	$\sigma_{t\parallel}$	50	1.8	0.3	50	1.8	0.5									
Mahogany	σ_b	50	3.3	0.6	50	3.4	0.6	50	2.0	0.4	50	2.9	0.5			
	$\sigma_{c\parallel}$	50	2.7	1.2	50	2.4	1.1									
	$\sigma_{c\perp}$	50	3.8	1.2	50	3.7	1.2	50	2.2	1.0	48	2.8	2.0			
	τ_{\parallel}	50	2.5	0.4	50	2.4	0.4									
	$\sigma_{t\parallel}$	50	2.0	0.3	50	2.0	0.3									
Red Meranti	σ_b	50	3.7	0.6	50	3.7	0.6	50	2.2	0.4	50	3.2	0.5			
	$\sigma_{c\parallel}$	50	2.6	0.7	50	2.4	0.7									
	$\sigma_{c\perp}$	50	2.7	0.3	50	2.7	0.3	50	1.4	0.2	45	1.9	0.4			
	τ_{\parallel}	51	2.3	0.4	51	2.2	0.5									
	$\sigma_{t\parallel}$	50	2.1	0.4	50	2.0	0.5									
Pine	σ_b	50	3.6	0.6	50	3.7	0.6	50	2.2	0.5	50	3.2	0.6			
	$\sigma_{c\parallel}$	50	2.7	0.8	50	2.5	0.7									
	$\sigma_{c\perp}$	50	3.3	0.6	50	3.3	0.6	50	1.9	0.5	47	2.3	0.7			
	τ_{\parallel}	50	2.8	0.9	50	2.8	0.9									
	$\sigma_{t\parallel}$	50	2.0	0.4	50	1.9	0.5									

Note: The ductility ratio for bamboo scrimber and wood subjected to: σ_b = static bending $\sigma_{t\parallel}$ = tension parallel-to-fiber, $\sigma_{c\parallel}$ = compression parallel-to-fiber, $\sigma_{c\perp}$ = compression perpendicular-to-fiber, τ_{\parallel} = shear parallel-to-fiber.

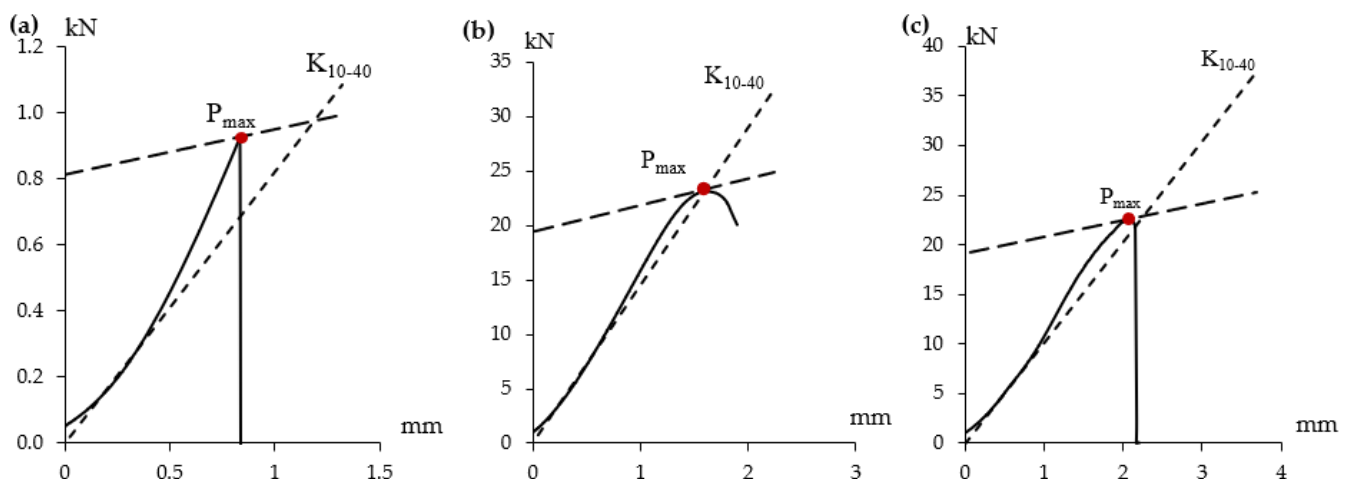


Figure 10. Examples the failure of K_{10-40} line that located offsite the load-displacement curve in (a) tension, (b) compression parallel-to-fiber, and (c) shear tests.

Figure 11 shows a representative diagram of the position of the yield point in all mechanical tests of bamboo scrimber. In scrimber, the yield load estimated using CEN and EEEP methods was significantly higher, and the lowest yield load value was estimated using CSIRO or K&C methods. However, the CEN and EEEP yield points are outside the load-displacement curve. The point of intersection between the initial stiffness and the tangent with a slope equal to one-sixth of the initial stiffness determines the yield point estimated using the CEN method. However, it is because the displacement at yield is not directly related to the actual

behavior. In other words, CEN and EEEP procedures do not reflect the point on the actual load-displacement curve of the specimen. In contrast to the Y&K method, which projected the yield point horizontally onto the load-displacement curve.

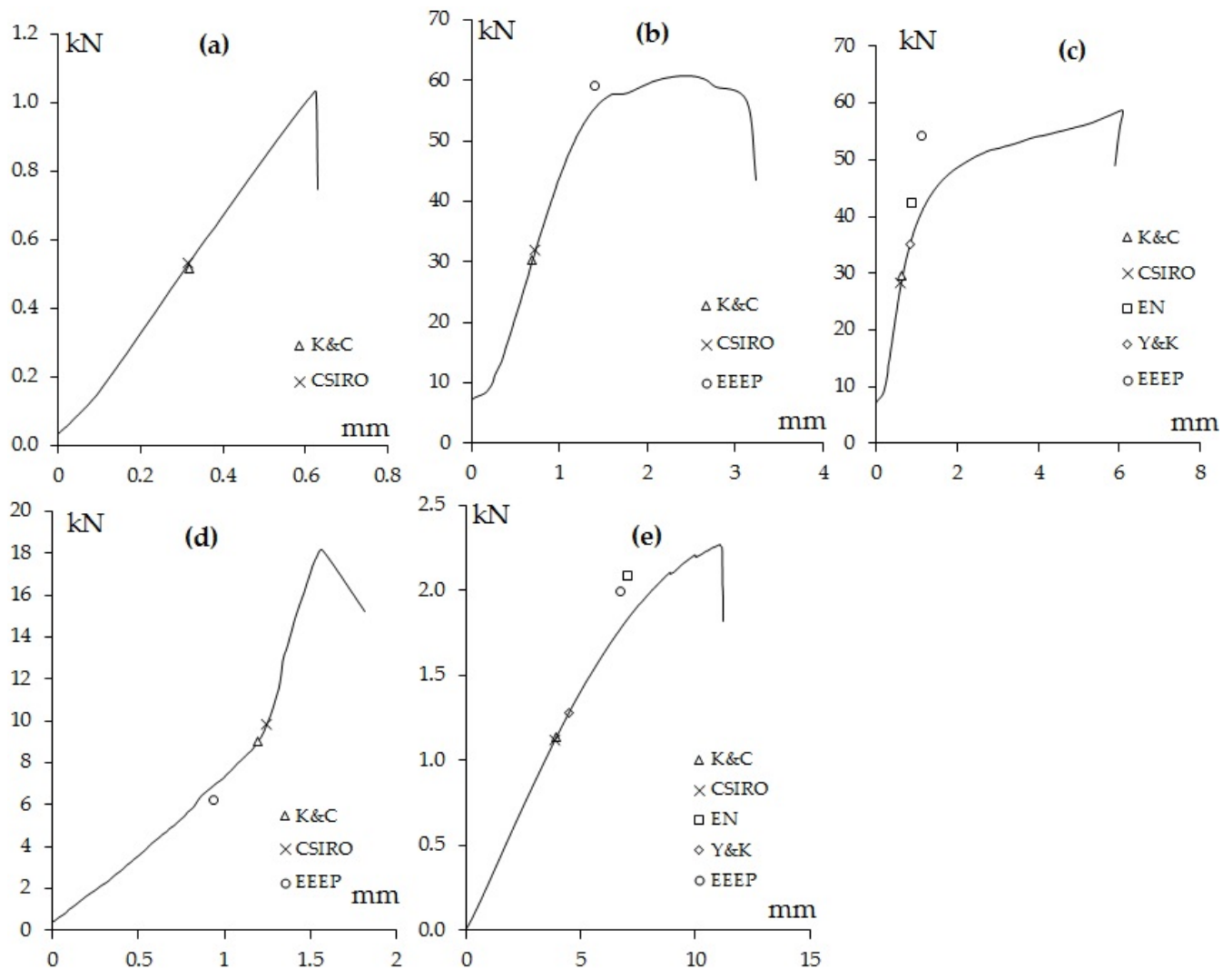


Figure 11. Position of yield points on the load-deformation curve of (a) tension parallel-to-fiber, (b) compression parallel-to-fiber, (c) compression perpendicular-to-fiber, (d) shear, and (e) flexural in bamboo scrimber.

Therefore, the given yield point reflects the actual point, unlike the CEN method [71]. The Y&K method, according to Munoz et al. [50], provided a better estimate of the yield load and can be well balanced by a second independent slope representing the elastic back zone. The intersection of the slope and its projection on the load-deformation curve provides the actual yield point.

The ductility ratio ranges in this experimental study were 0.03–19.74 and can be classified from low to high according to Eurocode 8 [39]. In contrast, according to Smith [72], it can be classified from brittle to high ductility (Table 5). The mean ductility ratio value of bamboo scrimber ranged between low to high, while in timber, the overall mean values of ductility ratio obtained from various mechanical properties are low. The ductility ratio of bamboo scrimber subjected to compression had the highest μ than timber, which can be classified as low to medium for compression parallel-to-fiber and medium to high for compression perpendicular-to-fiber. Although bamboo scrimber had the highest μ in compression, bamboo scrimber overall had the lowest μ of all specimens tested, other than

compression, which can be classified as low to medium ductility. This indicates that the displacement or plastic area before failure in bamboo scrimber is smaller than in timber. This behavior can be seen from the load-displacement curve of bamboo scrimber in the bending test, in which after reaching the yield point, the load continues to increase with a relatively small displacement and then reaches the maximum load (P_{max}), causing the specimen's failure.

Bamboo scrimber specimens reach their maximum load before timber specimens (e.g., pine) reach the maximum load (Figure 12). Chen et al. [29] studied the flexural ductility of Moso bamboo, which was 3.06 times higher than wood. The mean flexural ductility factor of Moso bamboo is 6.48, while the flexural ductility of bamboo scrimber in this experimental study ranges between 2.25 and 3.42. The contrast to the result in this study could be caused by bamboo as a raw material of bamboo scrimber that has undergone a compression process under high temperature and pressure [65], so it becomes denser than the untreated one. Obataya et al. [73] pointed out that the excellent bending ductility of bamboo is attributed to the combination of fiber-rich outer and compressible inner parts. In contrast, in bamboo scrimber, the outer part of natural round bamboo has been removed. However, the ductility ratio of bamboo scrimber in this study is comparable to bamboo scrimber strengthening timber beams with CFRP/wooden pin anchorage reported by Chen et al. [74], in which the value ranged between 1.08 and 3.35.

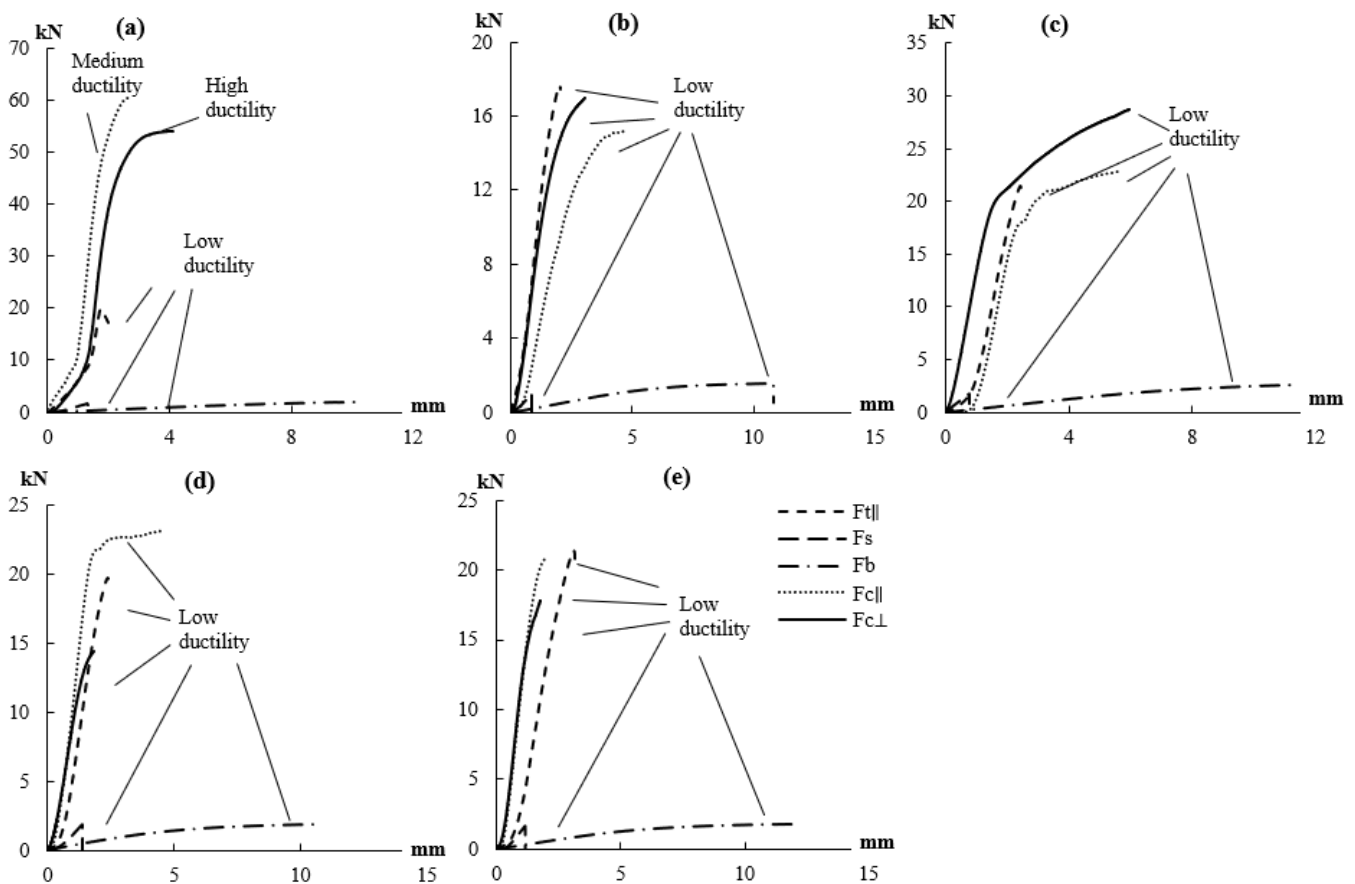


Figure 12. Load-displacement curve of mechanical properties tested in (a) bamboo scrimber, (b) agathis, (c) mahogany, (d) red meranti, and (e) pine.

Generally, the lowest ductility ratio of all mechanical properties tested was found in the tension parallel-to-fiber test. In contrast, the highest ductility ratio was found in the bending test for timber and compression parallel to the fiber of bamboo scrimber. In the bending test, the specimen will undergo deflection before the specimen failure. While in the tension parallel-to-fiber test, the specimen had little or no deflection and immediately

reached failure. The same behavior was also found in the CLT connection studied by Ceallaigh and Harte [75], that shear forces are more ductile than tensile. For connection subjected to a shearing force, significant deformation occurs before failure occurs after the yield point. Connections in tension forces are less ductile than in shear forces, and the load will drop significantly after reaching the maximum load. Similar behavior is also found in this study, shown in Figure 5a. The ductility behavior of bamboo scrimber in compression perpendicular-to-fiber can be categorized as high. Meanwhile, the ductility behavior in compression parallel-to-fiber is medium. However, bamboo scrimber subjected to bending, tension, and shear is low ductility or brittle. Smith and Asiz [76] concluded that typical range responses for components in structural timber systems illustrated in Jorissen and Fragiaco's [70] report are brittle for tension and bending members and ductile for compression both parallel and perpendicular-to-fiber.

Table 5. Classification of ductility ratio.

Classification	Ductility Ratio [72]	Ductility Ratio [77]
Brittle	$\mu \leq 2$	—
Low ductility	$2 < \mu \leq 4$	$\mu \leq 4$
Moderate ductility	$4 < \mu \leq 6$	$4 < \mu \leq 6$
High ductility	$\mu > 6$	$\mu > 6$

Bamboo scrimber is high ductility ($\mu > 6$) when subjected to compression perpendicular-to-fiber, medium ductility ($4 < \mu \leq 6$) when subjected to compression parallel-to-fiber, and low ductility (brittle) when subjected to bending, shear, or tensile parallel-to-fiber. The higher bamboo scrimber's ductility may give an alert and more time before failure than timbers. Timbers have brittle to lower ductility when receiving each kind of loading scheme.

3.5. Relationship between Ductility and Ratio of Stiffness to Strength

The correlations between the parameters describing the ratio of stiffness to strength with ductility are illustrated in Figure 13. The determination coefficients of linear regression (R^2) assumed values vary from 0.0011 to 0.2933 for timber specimens and 0.0017 to 0.7007 for scrimber specimens. The low value of R^2 in the correlation between E_b/σ_b and $E_{c\perp}/\sigma_{cp\perp}$ with ductility ratio for both timber and scrimber means that the ratio of stiffness to strength, in this case for E_b/σ_b and $E_{c\perp}/\sigma_{cp\perp}$, is independent of the ductility. While the ratio of shear modulus to shear strength ($G/\tau_{//}$) and compression modulus to strength modulus parallel-to-fiber ($E_{c\parallel}/\sigma_{c\parallel}$) significantly correlate to its ductility.

As mentioned above, red meranti has the highest E_b and σ_b value among all tested specimens. Red meranti also has the highest E_b/S_R value. Figure 13a shows that the ductility ratio of bamboo scrimber and timber has a positive correlation to E_b/S_R value. In compression, both parallel and perpendicular-to-fiber, the ratio between compression modulus and compression strength is negatively correlated to the ductility ratio of timber specimens, while in bamboo scrimber, vice versa. This kind of behavior also can be seen in the ratio between shear modulus and shear strength ($G/\tau_{//}$), which is negatively correlated to the ductility ratio of bamboo scrimber specimens. On the contrary, the correlation between timber's ($G/\tau_{//}$) and ductility ratio is positive.

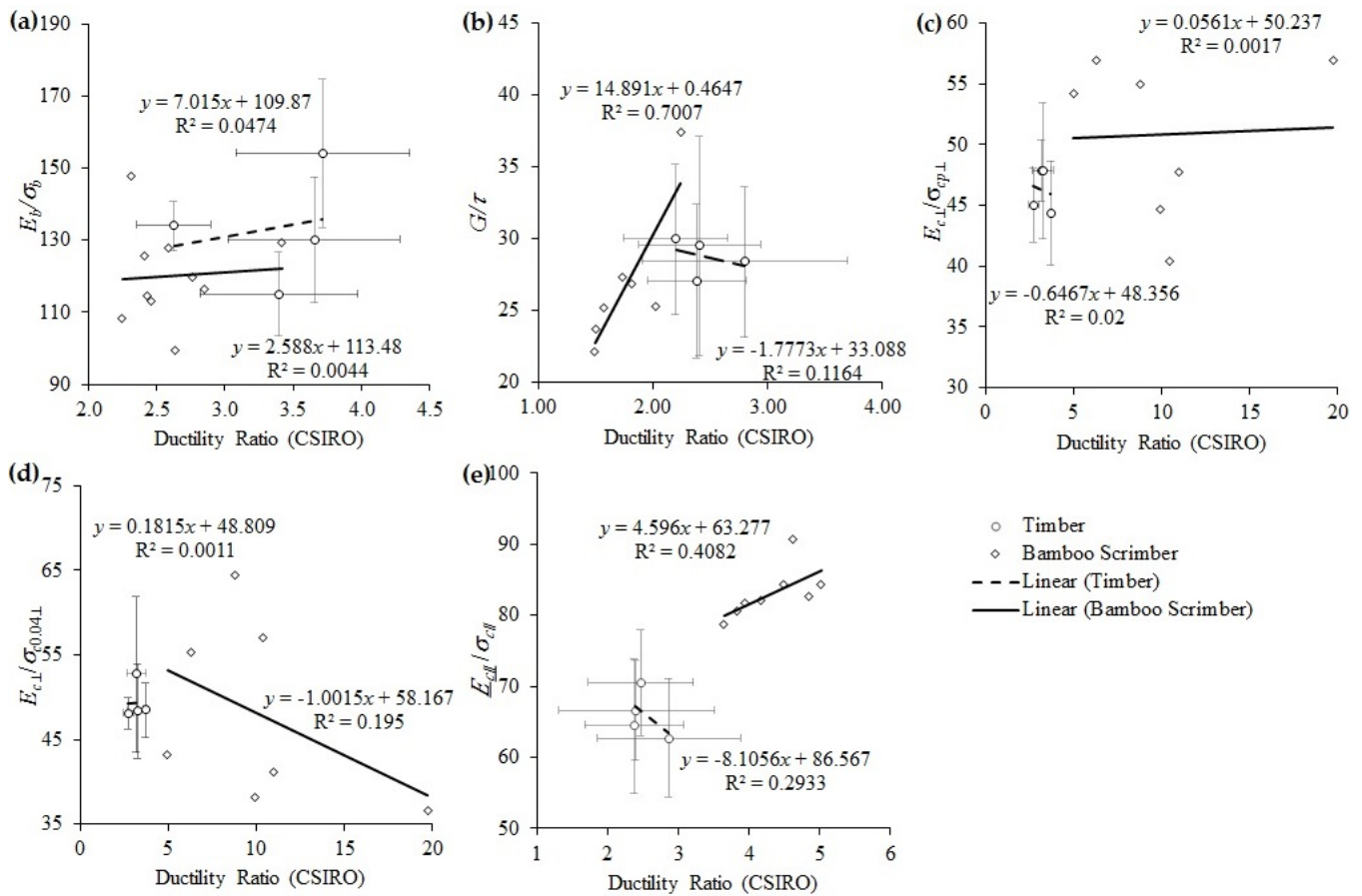


Figure 13. Linear regression between (a) E_b/σ_b , (b) G/τ , (c) $E_{c\perp}/\sigma_{cp\perp}$, (d) $E_{c\perp}/\sigma_{c0.04\perp}$, (e) $E_{c\parallel}/\sigma_{c\parallel}$ vs. ductility ratio.

4. Conclusions

Bamboo scrimber has a higher density than timber. Its drier equilibrium moisture contents indicate that scrimber is more hydrophobic than timbers. The maximum crushing strength ($\sigma_{c\parallel}$), compressive stress perpendicular-to-fiber at the proportional limit ($\sigma_{cp\perp}$) and at the 0.04" deformation ($\sigma_{c0.04\perp}$), shear strength (τ_{\parallel}), compressive longitudinal modulus of elasticity ($E_{c\parallel}$), compressive lateral modulus of elasticity ($E_{c\perp}$), and modulus of rigidity (G) of scrimber are higher than those of timbers. Both scrimber's and timber's flexural properties (modulus of rupture (σ_b) and flexural modulus of elasticity (E_b)) are comparable. On the contrary, the tensile strength parallel-to-fiber ($\sigma_{t\parallel}$) of scrimber is weaker than that of timber.

Bamboo scrimber is high ductility ($\mu > 6$) when subjected to compression perpendicular-to-fiber, medium ductility ($4 < \mu \leq 6$) when subjected to compression parallel-to-fiber, and low ductility (brittle) when subjected to bending, shear, or tensile parallel-to-fiber. The higher scrimber's ductility may give an alert and more time before failure than timbers. Timbers have brittle to low ductility when receiving each kind of loading scheme. The ratio of shear modulus to shear strength (G/τ_{\parallel}) and compression modulus to strength modulus parallel-to-fiber ($E_{c\parallel}/\sigma_{c\parallel}$) strongly correlate with the ductility ratio. However, the ratio of elasticity to rupture modulus (E_b/σ_b) and the ratio of compression perpendicular-to-fiber modulus to strength ($E_{c\perp}/\sigma_{cp\perp}$) are independent of the ductility value.

Author Contributions: Conceptualization, E.T.B. and N.N.; data curation, S.P.S. and E.T.B.; formal analysis, S.P.S. and E.T.B.; funding acquisition, N.N.; investigation, S.P.S. and E.T.B.; methodology, S.P.S., E.T.B. and N.N.; project administration, E.T.B. and N.N.; resources, N.N.; supervision, E.T.B. and N.N.; validation, S.P.S., E.T.B. and N.N.; visualization, S.P.S., E.T.B. and N.N.; writing—original

draft, S.P.S., E.T.B. and N.N.; writing—review and editing, E.T.B. and N.N. All authors have read and agreed to the published version of the manuscript.

Funding: The APC was funded by Collaborative Research Fund, Faculty of Forestry and Environment—IPB University.

Institutional Review Board Statement: Not applicable.

Informed Consent Statement: Not applicable.

Data Availability Statement: The data that support the findings of this study are available from the corresponding author, N.N., upon reasonable request.

Acknowledgments: The authors express their gratitude and appreciation to IPB University (Bogor Agricultural University) (ID) and the Directorate General of Higher Education—Ministry of Education, Culture, Research, and Technology (ID) for the finances, facilities, and opportunity to conduct this research.

Conflicts of Interest: The authors declare no conflict of interest.

Abbreviation

b	specimen width (mm)
d	specimen depth (mm)
E_b	modulus of elasticity (MPa)
$E_{C\parallel}$	modulus Young in compression parallel-to-fiber (MPa)
$E_{c\perp}$	modulus Young in compression perpendicular-to-fiber (MPa)
G	shear modulus (MPa)
G_b	specific gravity
L	specimen length (mm)
m_0	mass before testing (g)
m_1	mass after testing (g)
m_2	oven-dried mass (g)
M_c	moisture content (%)
$P_{0.04}$	load at 0.04 inch (N)
P_{max}	maximum load (N)
P_u	ultimate load (N) = maximum load (N)
P_p	load at proportional limit (N)
S_R	modulus of rupture (MPa)
<i>Greek symbol</i>	
μ	ductility ratio
Δ_u	ultimate displacement (mm)
Δ_y	yield displacement (mm)
ρ	density (g/cm ³)
τ	shear stress
γ	shear strain
σ	stress
$\sigma_{C\parallel}$	compressive strength parallel-to-fiber (MPa)
$\sigma_{c0.04\perp}$	compressive stress perpendicular-to-fiber at the 0.04 inch deformation (MPa)
$\sigma_{cp\perp}$	compressive stress perpendicular-to-fiber at the proportional limit (MPa)
τ_{\parallel}	shear strength parallel-to-fiber (MPa)
$\sigma_{t\parallel}$	tensile strength parallel-to-fiber (MPa)
ε	strain

References

1. Firmanti, A.; Bahtiar, E.T.; Surjokusumo, S.; Komatsu, K.; Kawai, S. Mechanical stress grading of tropical timbers without regard to species. *J. Wood Sci.* **2005**, *51*, 339–347. [[CrossRef](#)]
2. Bahtiar, E.T.; Nugroho, N.; Hermawan, D.; Wirawan, W.; Khuschandra. Triangle bracing system to reduce the vibration level of cooling tower—Case study in PT Star Energy Geothermal (Wayang Windu) Ltd.—Indonesia. *Case Stud. Constr. Mater.* **2018**, *8*, 248–257. [[CrossRef](#)]
3. Bahtiar, E.T.; Nugroho, N.; Rahman, M.M.; Arinana; Sari, R.K.; Wirawan, W.; Hermawan, D. Estimation the remaining service-lifetime of wooden structure of geothermal cooling tower. *Case Stud. Constr. Mater.* **2017**, *6*, 91–102. [[CrossRef](#)]
4. Bahtiar, E.T.; Erizal, E.; Hermawan, D.; Nugroho, N.; Hidayatullah, R. Experimental Study of Beam Stability Factor of Sawn Lumber Subjected to Concentrated Bending Loads at Several Points. *Forests* **2022**, *13*, 1480. [[CrossRef](#)]
5. Bahtiar, E.T.; Denih, A.; Priadi, T.; Putra, G.R.; Koswara, A.; Nugroho, N.; Hermawan, D. Comparing the Building Code Sawn Lumber's Wet Service Factors (CM) with Four Commercial Wood Species Laboratory Tests. *Forests* **2022**, *13*, 2094. [[CrossRef](#)]
6. Cahyono, T.D.; Wahyudi, I.; Priadi, T.; Febrianto, F.; Darmawan, W.; Bahtiar, E.T.; Ohorella, S.; Novriyanti, E. The quality of 8 and 10 years old samama wood (*Anthocephalus macrophyllus*). *J. Indian Acad. Wood Sci.* **2015**, *12*, 22–28. [[CrossRef](#)]
7. Bahtiar, E.T.; Arinana; Nugroho, N.; Nandika, D. Daily Cycle of Air Temperature and Relative Humidity Effect to Creep Deflection of Wood Component of Low-cost House in Cibeureum-Bogor, West Java, Indonesia. *Asian J. Sci. Res.* **2014**, *7*, 501–512. [[CrossRef](#)]
8. Hayatunnufus, A.; Nugroho, N.; Bahtiar, E.T. Faktor Stabilitas Balok Kayu pada Konfigurasi Pembebanan Terpusat (Stability Factor of Wooden Beams in One Point Loading). *J. Tek. Sipil Lingkungan.* **2022**, *7*, 129–146. [[CrossRef](#)]
9. Wang, C.; Zhang, H.; Zhao, C.; Zhang, C.; Cao, T.; Dong, H.; Ding, J.; Xiong, Z.; Xiong, X.; Liu, W.; et al. Experimental study on laminated bamboo lumber column; E3S Web of Conferences. In Proceedings of the 2018 4th International Conference on Energy Materials and Environment Engineering (ICEMEE 2018), Semenyih, Malaysia, 13–15 April 2018; Volume 38, pp. 1–5.
10. Nurmadina; Nugroho, N.; Bahtiar, E.T. Structural grading of *Gigantochloa apus* bamboo based on its flexural properties. *Constr. Build. Mater.* **2017**, *157*, 1173–1189. [[CrossRef](#)]
11. Bahtiar, E.T.; Imanullah, A.P.; Hermawan, D.; Nugroho, N.; Abdurachman. Structural grading of three sympodial bamboo culms (Hitam, Andong, and Tali) subjected to axial compressive load. *Eng. Struct.* **2019**, *181*, 233–245. [[CrossRef](#)]
12. Nugroho, N.; Bahtiar, E.T.; Nurmadina. Grading Development of Indonesian Bamboo Culm: Case Study on Tali Bamboo (*Gigantochloa apus*). In Proceedings of the 2018 World Conference on Timber Engineering, Seoul, Republic of Korea, 20–23 August 2018; pp. 1–6.
13. Nugroho, N.; Bahtiar, E.T. Buckling formulas for designing a column with *Gigantochloa apus*. *Case Stud. Constr. Mater.* **2021**, *14*, e00516. [[CrossRef](#)]
14. Nugroho, N.; Kartini; Bahtiar, E.T. Cross-species bamboo grading based on flexural properties. *IOP Conf. Ser. Earth Environ. Sci.* **2021**, *891*, 012008. [[CrossRef](#)]
15. Bahtiar, E.T.; Malkowska, D.; Trujillo, D.; Nugroho, N. Experimental study on buckling resistance of *Guadua angustifolia* bamboo column. *Eng. Struct.* **2021**, *228*, 111548. [[CrossRef](#)]
16. Bahtiar, E.T.; Trujillo, D.; Nugroho, N. Compression resistance of short members as the basis for structural grading of *Guadua angustifolia*. *Constr. Build. Mater.* **2020**, *249*, 118759. [[CrossRef](#)]
17. Cahyono, T.D.; Novriyanti, E.; Bahtiar, E.T.; Massijaya, M.Y. Development of composite beams made from tali (*Gigantochloa apus*) and hitam bamboo (*Gigantochloa atroviolacea*). *J. Indian Acad. Wood Sci.* **2014**, *11*, 156–161. [[CrossRef](#)]
18. Bahtiar, E.T.; Denih, A.; Karlinasari, L.; Putra, G.R.; Nugroho, N.; Sulistyono, S. Mengidealisasikan Penampang Lintang Buluh Bambu Menjadi Bentuk Geometri Conic Untuk Menghitung Sifat Penampangnya (Conic Geometric Idealization Shape of Bamboo Culm's Cross-section to Calculating Section Properties). *J. Penelit. Has. Hutan* **2022**, *40*, 165–188, The paper is still under processing.
19. Fridiyanti, I.; Massijaya, M.Y. Physical and mechanical properties of parallel strand lumber made from hot pre-pressed long strand oil palm trunk waste. *IOP Conf. Ser. Earth Environ. Sci.* **2018**, *141*, 012007. [[CrossRef](#)]
20. Bahtiar, E.T.; Nugroho, N.; Surjokusumo, S. Estimating Young's Modulus and Modulus of Rupture of Coconut Logs using Reconstruction Method. *Civ. Eng. Dimens.* **2010**, *12*, 65–72. [[CrossRef](#)]
21. Hermawan, D.; Budiman, I.; Febrianto, F.; Subyakto, S.; Pari, G.; Ghozali, M.; Bahtiar, E.T.; Sutiawan, J.; de Azevedo, A.R.G. Enhancement of the Mechanical, Self-Healing and Pollutant Adsorption Properties of Mortar Reinforced with Empty Fruit Bunches and Shell Chars of Oil Palm. *Polymers* **2022**, *14*, 410. [[CrossRef](#)]
22. Sinha, A.; Way, D.; Mlasko, S. Structural Performance of Glued Laminated Bamboo Beams. *J. Struct. Eng.* **2014**, *140*, 04013021. [[CrossRef](#)]
23. Xiao, Y.; Shan, B.; Yang, R.Z.; Li, Z.; Chen, J. Glue Laminated Bamboo (GluBam) for Structural Applications. In *Materials and Joints in Timber Structures*; Springer: Dordrecht, The Netherlands, 2014; pp. 589–601.
24. Alam, D.; Rahman, K.-S.; Ratul, S.; Sharmin, A.; Islam, T.; Hasan, M.; Islam, M. Properties of Particleboard Manufactured from Commonly Used Bamboo (*Bambusa vulgaris*) Wastes in Bangladesh. *Adv. Res.* **2015**, *4*, 203–211. [[CrossRef](#)]
25. Marinho, N.P.; do Nascimento, E.M.; Nisgoski, S.; de Valarelli, I.D. Some physical and mechanical properties of medium-density fiberboard made from giant bamboo. *Mater. Res.* **2013**, *16*, 1387–1392. [[CrossRef](#)]
26. Febrianto, F.; Sahroni; Hidayat, W.; Bakar, E.S.; Kwon, G.-J.; Kwon, J.-H.; Hong, S.-I.; Kim, N.-H. Properties of oriented strand board made from Betung bamboo (*Dendrocalamus asper* (Schultes.f) Backer ex Heyne). *Wood Sci. Technol.* **2012**, *46*, 53–62. [[CrossRef](#)]

27. Huang, Z.; Sun, Y.; Musso, F. Assessment on bamboo scrimber as a substitute for timber in building envelope in tropical and humid subtropical climate zones—Part 1 hygrothermal properties test. *IOP Conf. Ser. Mater. Sci. Eng.* **2017**, *264*, 012006. [[CrossRef](#)]
28. Liu, X.; Smith, G.D.; Jiang, Z.; Bock, M.C.D.; Boeck, F.; Frith, O.; Gatóo, A.; Liu, K.; Mulligan, H.; Semple, K.E.; et al. Nomenclature for engineered bamboo. *BioResources* **2016**, *11*, 1141–1161. [[CrossRef](#)]
29. Chen, J.; Guagliano, M.; Shi, M.; Jiang, X.; Zhou, H. A comprehensive overview of bamboo scrimber and its new development in China. *Eur. J. Wood Wood Prod.* **2020**, *79*, 363–379. [[CrossRef](#)]
30. Sun, X.; He, M.; Li, Z. Novel engineered wood and bamboo composites for structural applications: State-of-art of manufacturing technology and mechanical performance evaluation. *Constr. Build. Mater.* **2020**, *249*, 118751. [[CrossRef](#)]
31. Zou, Z.; Wu, J.; Zhang, X. Influence of Moisture Content on Mechanical Properties of Bamboo Scrimber. *J. Mater. Civ. Eng.* **2019**, *31*, 06019004. [[CrossRef](#)]
32. Van der Lugt, P. *Design Interventions for Stimulating Bamboo Commercialization—Dutch Design Meets Bamboo as a Replicable Model*; VSSD: Kanpur, India, 2008; ISBN 9789051550474.
33. Kumar, A.; Ryparovà, P.; Kasal, B.; Adamopoulos, S.; Hajek, P. Resistance of bamboo scrimber against white-rot and brown-rot fungi. *Wood Mater. Sci. Eng.* **2018**, *15*, 57–63. [[CrossRef](#)]
34. Shangquan, W.; Zhong, Y.; Xing, X.; Zhao, R.; Ren, H. 2D model of strength parameters for Bamboo scrimber. *BioResources* **2014**, *9*, 7073–7085. [[CrossRef](#)]
35. Kumar, A.; Vlach, T.; Laiblova, L.; Hrouda, M.; Kasal, B.; Tywoniak, J.; Hajek, P. Engineered bamboo scrimber: Influence of density on the mechanical and water absorption properties. *Constr. Build. Mater.* **2016**, *127*, 815–827. [[CrossRef](#)]
36. Huang, Y.; Ji, Y.; Yu, W. Development of bamboo scrimber: A literature review. *J. Wood Sci.* **2019**, *65*, 25. [[CrossRef](#)]
37. Sharma, B.; Gatóo, A.; Bock, M.; Ramage, M. Engineered bamboo for structural applications. *Constr. Build. Mater.* **2015**, *81*, 66–73. [[CrossRef](#)]
38. Kirkegaard, P.H.; Sørensen, J.D.; Cizmar, D.; Rajčić, V. Robustness analysis of a wide-span timber structure with ductile behaviour. In Proceedings of the Tenth International Conference on Computational Structures Technology, Valencia, Spain, 14–17 September 2010; Volume 93.
39. *EN 1998-1*; Eurocode 8: Design of Structures for Earthquake Resistance. The European Union: Brussels, Belgium, 2005.
40. Mander, J.B.; Basoz, N. Seismic fragility curve theory for highway bridges. In *Optimizing Post-Earthquake Lifeline System Reliability*; ASCE: Reston, VA, USA, 1999; pp. 31–40.
41. Popovski, M.; Gavric, I.; Coe, I. Performance of Two-Storey CLT House Subjected to Lateral Loads. In Proceedings of the World Conference on Timber Engineering, Quebec City, QC, Canada, 10–14 August 2014.
42. Gavric, I.; Fragiaco, M.; Ceccotti, A. Cyclic Behavior of CLT Wall Systems: Experimental Tests and Analytical Prediction Models. *J. Struct. Eng.* **2015**, *141*, 04015034. [[CrossRef](#)]
43. Fragiaco, M.; Amadio, C.; Sancin, L.; Rinaldin, G. Seismic analysis of a light-frame timber building with and without friction pendulum base isolation. In Proceedings of the World Conference of Timber Engineering WCTE, Auckland, New Zealand, 15–19 July 2012.
44. Chen, M.; Ye, L.; Li, H.; Wang, G.; Chen, Q.; Fang, C.; Dai, C.; Fei, B. Flexural strength and ductility of moso bamboo. *Constr. Build. Mater.* **2020**, *246*, 118418. [[CrossRef](#)]
45. Ahmad, Y. Ductility of Timber Beams Strengthened Using Fiber Reinforced Polymer. *J. Civ. Eng. Archit.* **2013**, *7*, 535–544. [[CrossRef](#)]
46. Baduge, S.K.; Mendis, P.; Ngo, T.D.; Sofi, M. Ductility Design of Reinforced Very-High Strength Concrete Columns (100–150 MPa) Using Curvature and Energy-Based Ductility Indices. *Int. J. Concr. Struct. Mater.* **2019**, *13*, 37. [[CrossRef](#)]
47. Tomasi, R.; Parisi, M.A.; Piazza, M. Ductile Design of Glued-Laminated Timber Beams. *Pract. Period. Struct. Des. Constr.* **2009**, *14*, 113–122. [[CrossRef](#)]
48. Newcombe, M.P.; Pampanin, S.; Buchanan, A.; Palermo, A. Section Analysis and Cyclic Behavior of Post-Tensioned Jointed Ductile Connections for Multi-Story Timber Buildings. *J. Earthq. Eng.* **2008**, *12*, 83–110. [[CrossRef](#)]
49. Livas, C.; Ekevad, M.; Öhman, M. Experimental analysis of passively and actively reinforced glued-laminated timber with focus on ductility. *Wood Mater. Sci. Eng.* **2021**, *17*, 129–137. [[CrossRef](#)]
50. Muñoz, W.; Salenikov, A.; Mohammad, M.; Quenneville, P. Determination of yield point and ductility of timber assemblies: In search for a harmonised approach. In Proceedings of the 10th World Conference on Timber Engineering 2008, Miyazaki, Japan, 2–5 June 2008.
51. Sharma, B.; Van Der Vegte, A. *Engineered Bamboo for Structural Applications*; Elsevier Ltd.: Amsterdam, The Netherlands, 2019; ISBN 9780081027042.
52. *ASTM D143-14*; Standard Test Methods for Small Clear Specimens of Timber. American Society for Testing and Materials (ASTM): West Conshohocken, PA, USA, 2014.
53. Karacabeyli, E.; Ceccotti, A. Nailed Wood-Frame Shear Walls for Seismic Loads: Test Results and Design Considerations. In Structural Engineering World Wide 1998, Proceedings of the Structural Engineering World Congress, San Francisco, CA, USA, 18–23 July 1998; Elsevier: Amsterdam, The Netherlands, 1999; pp. 1–9.
54. Foliente, G.C.; Leicester, R.H. Evaluation of mechanical joint systems in timber structures. In Proceedings of the 25th Forest Products Research Conference, Melbourne, Australia, 18–21 November 1996; p. 2/16. Available online: <http://hdl.handle.net/10.2.100.100/228051?index=1> (accessed on 10 December 2022).

55. Gnanaharan, R.; Janssen, J.; Arce, O. *Bending Strength of Bamboo: Comparison of Different Testing Procedures with a View to Standardization*; International Network for Bamboo and Rattan: New Delhi, India, 1994.
56. Yasumura, M.; Kawai, N. Estimating seismic performance of wood-framed structures. In Proceedings of the 5th World Conference on Timber Engineering, Montreux, Switzerland, 17–20 August 1998; Volume 2.
57. Foliente, G. Issues in seismic performance testing and evaluation of timber structural systems. In Proceedings of the 1996 International Wood Engineering Conference, New Orleans, LA, USA, 28–31 October 1996; pp. 29–36.
58. Terauchi, F.; Mulyono, A.; Tauchi, T.; Kubo, M. Typological Analysis of Engineered Bamboo Product Surfaces. *J. Sci. Des.* **2019**, *3*, 1_69–1_76. [[CrossRef](#)]
59. Bahtiar, E.T.; Nugroho, N.; Massijaya, M.Y.; Roliandi, H.; Rentry, A.N.; Satriawan, A. A new method to estimate modulus of elasticity and modulus of rupture of glulam I-joist. *AIP Conf. Proc.* **2010**, *1325*, 319–322.
60. Bahtiar, E.T.; Nugroho, N.; Massijaya, M.Y.; Roliandi, H.; Augusti, R.; Satriawan, A. Method to Estimate Mechanical Properties of Glulam on Flexure Testing Based on Its Laminae Characteristics and Position. *Indones. J. Phys.* **2016**, *22*, 57–67. [[CrossRef](#)]
61. Nugroho, N.; Bahtiar, E.T.; Lelono, A.B. Kekuatan Bambu Betung (*Dendrocalamus asper* Backer ex K. Heyne) Menahan Gaya Normal Tekanan dan Tarikan (The Strength of Betung Bamboo (*Dendrocalamus asper* Backer ex K. Heyne) to Support Normal Force in Compression and Tension). *J. Penelit. Has. Hutan* **2022**, *40*, 37–48. [[CrossRef](#)]
62. Glass, S.V.; Zelinka, S.L. Moisture relations and physical properties of wood. In *Wood Handbook; Wood as an Engineering Material*; General Technical Report FPL-GTR-282; U.S. Department of Agriculture, Forest Service, Forest Products Laboratory: Madison, WI, USA, 2021.
63. Huang, D.; Bian, Y.; Zhou, A.; Sheng, B. Experimental study on stress-strain relationships and failure mechanisms of parallel strand bamboo made from phyllostachys. *Constr. Build. Mater.* **2015**, *77*, 130–138. [[CrossRef](#)]
64. Li, H.; Zhang, H.; Qiu, Z.; Su, J.; Wei, D.; Lorenzo, R.; Yuan, C.; Liu, H.; Zhou, C. Mechanical properties and stress strain relationship models for bamboo scrimber. *J. Renew. Mater.* **2020**, *8*, 13–27. [[CrossRef](#)]
65. Li, X.; Mou, Q.; Ren, H.; Li, X.; Zhong, Y. Effects of moisture content and load orientation on dowel-bearing behavior of bamboo scrimber. *Constr. Build. Mater.* **2020**, *262*, 120864. [[CrossRef](#)]
66. Li, H.; Zhang, Q.; Huang, D.; Deeks, A.J. Compressive performance of laminated bamboo. *Compos. Part B Eng.* **2013**, *54*, 319–328. [[CrossRef](#)]
67. Alipon, M.A.; Garcia, C.M.; Bondad, E.O. Glue and preservative effects on the properties and durability of engineered bamboo boards. *Philipp. J. Sci.* **2018**, *147*, 601–616.
68. Bodig, J.; Jayne, B. *Mechanics of Wood and Wood Composites*; Van Nostrand Reinhold: Washington, DC, USA, 1982; Volume 1.
69. Geiser, M.; Bergmann, M.; Follesa, M. Influence of steel properties on the ductility of doweled timber connections. *Constr. Build. Mater.* **2021**, *266*, 121152. [[CrossRef](#)]
70. Jorissen, A.; Fragiaco, M. General notes on ductility in timber structures. *Eng. Struct.* **2011**, *33*, 2987–2997. [[CrossRef](#)]
71. Brühl, F. *Ductility in Timber Structures—Possibilities and Requirements with Regard to Dowel Type Fasteners*; Institut für Konstruktion und Entwurf: Stuttgart, Germany, 2020.
72. Smith, I.; Asiz, A.; Snow, M.; Chui, Y. Possible Canadian/ISO approach to deriving design values from test data. In Proceedings of the CIB-W18, 39th Meeting, Florence, Italy, 28–31 August 2006.
73. Obataya, E.; Kitin, P.; Yamauchi, H. Bending characteristics of bamboo (*Phyllostachys pubescens*) with respect to its fiber–foam composite structure. *Wood Sci. Technol.* **2007**, *41*, 385–400. [[CrossRef](#)]
74. Chen, S.; Wei, Y.; Peng, D.; Zhao, K.; Hu, Y. Experimental investigation of timber beams strengthened by bamboo scrimber with anchorage structure. *Structures* **2021**, *33*, 1–11. [[CrossRef](#)]
75. Cealligh, C.O.; Harte, A.M. The elastic and ductile behaviour of CLT wall-floor connections and the influence of fastener length. *Eng. Struct.* **2019**, *189*, 319–331. [[CrossRef](#)]
76. Smith, I.; Asiz, A. Transition from design of timber components to design of system. In Proceedings of the IABSE-fib Conference, Cavtat, Croatia, 3–5 May 2010.
77. *EN 12512:2001; Timber Structures—Test Methods—Cyclic Testing of Joints Made with Mechanical Fasteners*. Comité Européen de Normalisation (CEN): Brussels, Belgium, 2005.

Disclaimer/Publisher’s Note: The statements, opinions and data contained in all publications are solely those of the individual author(s) and contributor(s) and not of MDPI and/or the editor(s). MDPI and/or the editor(s) disclaim responsibility for any injury to people or property resulting from any ideas, methods, instructions or products referred to in the content.